Journal of Engineering Mathematics 19 (1985) 233–246.

On flows with closed streamlines

E.W. HADDON and N. RILEY

Schools of Information Systems, and Mathematics and Phyics, University of East Anglia, Norwich, England

(Received April 10, 1985)

Summary

In this paper we present numerical solutions of the steady, two-dimensional Navier-Stokes equations for an incompressible fluid, for the flow in a plane elliptical region driven by the motion of its boundary. As the Reynolds number increases a core region in which the vorticity is uniform emerges, and a favourable comparison is possible with results obtained in the high-Reynolds-number limit.

1. Introduction

The well-known Prandtl-Batchelor theorem states that in an inviscid flow, regions in which there are closed streamlines are regions of the flow in which the vorticity is uniform, see for example Batchelor [1]. If the region of closed streamlines is enclosed by a solid boundary, and the fluid has vanishingly small viscosity, then it and the 'core' of uniform vorticity are separated by a thin boundary layer. In such a situation the flow will be driven by some part, or all, of the moving boundary and the role of the boundary layer is crucial in determining the core vorticity. In the simple case of a circular boundary the core vorticity is readily determined without reference to the details of the boundary-layer solution. In other situations the periodic boundary-layer solution will have to be known explicitly in order to determine the core vorticity. Riley [2] has considered such a situation in which the boundary of a plane elliptical region is in continuous motion. He shows that, with a finite computational domain, periodicity of the boundary-layer solution is not sufficient to determine the core vorticity uniquely. It is necessary, in addition, to ensure carefully that the boundary-layer and core vorticity match in an appropriate manner.

In the present paper we return to the steady flow of an incompressible, viscous fluid in an elliptical geometry in which the flow is driven by motion of the boundary. Our numerical solutions have been obtained at finite values of an appropriately defined Reynolds number by a method introduced by Dennis and Hudson [3], and the aims of our investigation are three-fold. The numerical method [3] is one which is second-order accurate in the grid sizes of the computational mesh with finite-difference equations that have associated matrices of diagonally-dominant form, without recourse to windward differencing. The method has been used with both rectangular [3] and polar [4] coordinates but its usefulness cannot be guaranteed in any particular coordinate system. One of our aims, therefore, is to demonstrate the applicability and effectiveness of this powerful method in an elliptic coordinate system. A second aim is to confirm, by a direct

comparison of results, that the method outlined in [2] is indeed an appropriate one in the high-Reynolds-number limit. A final aim is to extend the range of results to higher values of ellipse eccentricity than was apparently possible in [2], and in particular to reveal any anomalies in the flow that might account for the difficulties encountered in [2] at higher eccentricities.

In Section 2 we introduce the governing equations in split operator form and, following [3], the fairly elaborate discretisation of them that leads to sets of finite-difference equations with associated diagonally-dominant matrices. Section 3 deals with the numerical procedures associated with the iterative scheme and the results obtained are presented and discussed in Section 4. Results that have been obtained cover a range of ellipse eccentricities and Reynolds numbers. Our results show that as the Reynolds number increases a well-defined region emerges in the core of the flow in which the vorticity is uniform, as expected. We make a favourable comparison of this core vorticity with the results obtained in the high-Reynolds-number limit [2]. In the solutions for higher eccentricities than were apparently possible in [2] we see a substantial increase in the core vorticity, but otherwise report no unusual features of the flow.

2. Governing equations and finite-difference approximations

We are concerned with the steady, two-dimensional flow of an incompressible, viscous fluid that takes place inside, and in the plane of a cross-section of, the elliptic cylinder

$$\frac{x'^2}{a^2}+\frac{y'^2}{b^2}=1, \tag{2.1}$$

where (x', y') are rectangular coordinates and (a, b) the semi-major and -minor axes of the ellipse. We work with elliptic coordinates (ξ, η), related to the non-dimensional rectangular coordinates $(x, y)=(x'/l, y'/l)$ by

$$x = 2\,\mathrm{e}^{-\eta_e}\cosh\eta\cos\xi, \quad y = 2\,\mathrm{e}^{-\eta_e}\sinh\eta\sin\xi, \tag{2.2}$$

where $\eta=\eta_e$ represents the ellipse; the characteristic length l has been taken as $l=\frac{1}{2}a\,\mathrm{e}^{\eta_e}\operatorname{sech}\eta_e$ and the eccentricity of the ellipse is given by $e=\operatorname{sech}\eta_e$. The motion within the ellipse is induced by a 'slip' velocity at the boundary which we take, as in [2], to be

$$U_e = U_0\left(1+\tfrac{3}{4}\cos\xi\right), \tag{2.3}$$

where U_0 is some constant velocity. With scale $U_0 l$ we introduce the dimensionless stream function ψ which is related to the velocity components in the (ξ, η)-directions by

$$u=\frac{1}{s}\frac{\partial\psi}{\partial\eta}, \quad v=-\frac{1}{s}\frac{\partial\psi}{\partial\xi} \tag{2.4}$$

where, for the elliptic coordinates employed here the scale factors s_1, s_2 are equal and given by

$$s_1=s_2=s=2\,\mathrm{e}^{-\eta_e}\left(\sinh^2\eta+\sin^2\xi\right)^{1/2}. \tag{2.5}$$

We choose to work with the split-operator or (ψ, ζ)-form of the Navier-Stokes equations, where ζ is the vorticity, such that the governing equations are

$$\begin{aligned} \nabla^2\zeta &= R\left(\frac{\partial\psi}{\partial\eta}\frac{\partial\zeta}{\partial\xi} - \frac{\partial\psi}{\partial\xi}\frac{\partial\zeta}{\partial\eta}\right), \\ \nabla^2\psi &= -s^2\zeta, \end{aligned} \tag{2.6}$$

where $\nabla^2 = \partial^2/\partial\xi^2 + \partial^2/\partial\eta^2$ is the two-dimensional Laplacian, and $R = U_0 l/\nu$ is the Reynolds number, where ν is the kinematic viscosity. The boundary conditions that we require to satisfy on the ellipse are

$$\psi = 0 \qquad \text{on} \quad \eta = \eta_e, \tag{2.7}$$

together with a condition on ζ at $\eta = \eta_e$ which is derived from the velocity of slip in (2.3).

The governing equations, (2.6), are discretised on the (ξ, η) grid. A typical grid point on this grid has coordinates (ξ_0, η_0), and flow quantities there are denoted by subscript 0. At the adjacent grid points $(\xi_0 + h, \eta_0)$, $(\xi_0, \eta_0 + k)$, $(\xi_0 - h, \eta_0)$ and $(\xi_0, \eta_0 - k)$, quantities will be denoted by subscripts 1, 2, 3 and 4 respectively.

For equation $(2.6)_2$ the standard central-difference approximation yields, with $\lambda = h/k$,

$$\psi_1 + \lambda^2\psi_2 + \psi_3 + \lambda^2\psi_4 - 2(1+\lambda^2)\psi_0 + s_0^2 h^2 \zeta_0 = 0. \tag{2.8}$$

For the vorticity-transport equation the finite-difference method follows a derivation originating with Dennis [5]. We first use (2.4) to write $(2.6)_1$ as

$$\nabla^2\zeta = Rs\left(u\frac{\partial\zeta}{\partial\xi} + v\frac{\partial\zeta}{\partial\eta}\right), \tag{2.9}$$

which we then separate into the two equations

$$\begin{aligned} \frac{\partial^2\zeta}{\partial\xi^2} - Rsu\frac{\partial\zeta}{\partial\xi} &= A(\xi, \eta), \\ \frac{\partial^2\zeta}{\partial\eta^2} - Rsv\frac{\partial\zeta}{\partial\eta} &= -A(\xi, \eta), \end{aligned} \tag{2.10}$$

where $A(\xi, \eta)$ is an unknown function. Consider equation $(2.10)_1$. Along the ellipse $\eta = \eta_0$ we put

$$\zeta = F(\xi, \eta_0)\, \mathrm{e}^{-f(\xi, \eta_0)}, \tag{2.11}$$

where

$$f(\xi, \eta_0) = -\tfrac{1}{2}R\int_{\xi_0}^{\xi} s(t, \eta_0)u(t, \eta_0)\mathrm{d}t. \tag{2.12}$$

The equation for F is, from $(2.10)_1$

$$\frac{\partial^2 F}{\partial\xi^2} - \tfrac{1}{4}R^2s^2u^2F + \tfrac{1}{2}RF\frac{\partial}{\partial\xi}(su) = A\mathrm{e}^{f}, \tag{2.13}$$

where all partial derivatives are evaluated at $\eta = \eta_0$. Similarly along the hyperbola $\xi = \xi_0$ we put

$$\zeta = G(\xi_0, \eta)\, \mathrm{e}^{-g(\xi_0, \eta)}, \tag{2.14}$$

where

$$g(\xi_0, \eta) = -\tfrac{1}{2}R\int_{\eta_0}^{\eta} s(\xi_0, t)v(\xi_0, t)\mathrm{d}t, \tag{2.15}$$

and from $(2.10)_2$ G satisfies

$$\frac{\partial^2 G}{\partial \eta^2} - \tfrac{1}{4}R^2 s^2 v^2 G + \tfrac{1}{2}RG\frac{\partial}{\partial \eta}(sv) = -A\, \mathrm{e}^{g}, \tag{2.16}$$

where all partial derivatives are now evaluated at $\xi = \xi_0$.

We now approximate each of the equations (2.13) and (2.16) in terms of central differences at the point (ξ_0, η_0) where both equations are applicable. The quantity $A(\xi_0, \eta_0)$ may be eliminated to give, after replacing F, G in terms of ζ, and using (2.4),

$$\zeta_1\, \mathrm{e}^{f_1} + \zeta_3\, \mathrm{e}^{f_3} + \lambda^2\zeta_2\, \mathrm{e}^{g_2} + \lambda^2\zeta_4\, \mathrm{e}^{g_4} - \left\{2(1+\lambda^2) + \tfrac{1}{4}h^2R^2s_0^2\left(u_0^2 + v_0^2\right)\right\}\zeta_0 = 0. \tag{2.17}$$

Our approximation (2.17) of the vorticity transport equation has a truncation error $O(h^4) + O(h^2k^2)$ which is the same as if the equation had been discretised using standard central differences. The difference equations (2.8) and (2.17) are to be solved iteratively. Now, the matrix associated with (2.17) does not necessarily possess the desirable property of diagonal dominance as it stands. We therefore follow the method of Dennis and Hudson [3] to obtain a form of (2.17) that yields diagonal dominance without any further loss of accuracy.

If the integrand of (2.12) is expanded in a Taylor series, followed by a further expansion of the exponential function, it may readily be shown that

$$\mathrm{e}^{f_1} = 1 - \tfrac{1}{2}Rs_0u_0h + \tfrac{1}{8}R^2s_0^2u_0^2h^2 - \tfrac{1}{4}R\frac{\partial}{\partial \xi}(su)_0h^2 + O(h^3),$$

and (2.18)

$$\mathrm{e}^{f_3} = 1 + \tfrac{1}{2}Rs_0u_0h + \tfrac{1}{8}R^2s_0^2u_0^2h^2 - \tfrac{1}{4}R\frac{\partial}{\partial \xi}(su)_0h^2 + O(h^3),$$

with corresponding, similar, expressions for e^{g_2}, e^{g_4} following an expansion of (2.15). These quantities are introduced into (2.17) which is further simplified by the use of (2.4), and the observation that

$$\zeta_1 + \zeta_3 = 2\zeta_0 + O(h^2), \quad \zeta_2 + \zeta_4 = 2\zeta_0 + O(k^2),$$

$$\zeta_1 - \zeta_3 = O(h), \quad \zeta_2 - \zeta_4 = O(k),$$

together with the consistent neglect of terms $O(h^4, k^4)$ to give, finally,

$$c_1\zeta_1 + c_2\zeta_2 + c_3\zeta_3 + c_4\zeta_4 - c_0\zeta_0 = 0, \tag{2.19}$$

where

$$\begin{aligned} c_1 &= 1 - \tfrac{1}{2}Rs_0u_0h + \tfrac{1}{8}R^2s_0^2u_0^2h^2, \\ c_2 &= \lambda^2\left(1 - \tfrac{1}{2}Rs_0v_0k + \tfrac{1}{8}R^2s_0^2v_0^2k^2\right), \\ c_3 &= 1 + \tfrac{1}{2}Rs_0u_0h + \tfrac{1}{8}R^2s_0^2u_0^2h^2, \\ c_4 &= \lambda^2\left(1 + \tfrac{1}{2}Rs_0v_0k + \tfrac{1}{8}R^2s_0^2v_0^2k^2\right), \\ c_0 &= 2 + 2\lambda^2 + \tfrac{1}{4}h^2R^2s_0^2\left(u_0^2 + v_0^2\right). \end{aligned} \tag{2.20}$$

It is readily shown that for all values of u_0h and v_0k, $c_i > 0$, $i = 1$ to 4, and further, since

$$c_1 + c_2 + c_3 + c_4 = c_0,$$

it follows that the matrix associated with the set of equations (2.19) is diagonally dominant in the sense of Varga [6]. We also remark, again, that (2.19) is of the same order of accuracy with respect to the grid size as the approximation to (2.9) by central differences, but the actual error terms are quite different.

The remaining boundary condition that we must consider is a condition on the vorticity at the boundary $\eta = \eta_e$. The natural boundary condition to apply there is on the tangential velocity $(2.4)_1$ given in dimensionless form by $u_e = 1 + \frac{3}{4}\cos\xi$. In order to represent this as a condition on the vorticity ζ_e at the boundary we use a technique introduced by Woods [7], and employed extensively by Dennis and his co-workers (see for example [4]). First we write

$$\begin{aligned} \psi_2 &= \psi_1 - k\left(\frac{\partial\psi}{\partial\eta}\right)_1 + \tfrac{1}{2}k^2\left(\frac{\partial^2\psi}{\partial\eta^2}\right)_1 - \tfrac{1}{6}k^3\left(\frac{\partial^3\psi}{\partial\eta^3}\right)_1 + \ldots \\ &= -ks_1\left(1 + \tfrac{3}{4}\cos\xi_1\right) + \tfrac{1}{2}k^2\left(\frac{\partial^2\psi}{\partial\eta^2}\right)_1 - \tfrac{1}{6}k^3\left(\frac{\partial^3\psi}{\partial\eta^3}\right)_1 + \ldots, \end{aligned} \tag{2.21}$$

using the boundary condition on ψ and its derivative. Our notation in (2.21) is such that a subscript 1 now denotes a boundary point whilst a subscript 2 denotes the first grid point in from the boundary along a coordinate line and so on, bearing in mind that η increases outward. The term $O(k^2)$ may be evaluated from $(2.6)_2$ directly to give

$$\left(\frac{\partial^2\psi}{\partial\eta^2}\right)_1 = -s_1^2\zeta_1.$$

Differentiation of $(2.6)_2$ with respect to η allows us, after some manipulation, to evaluate

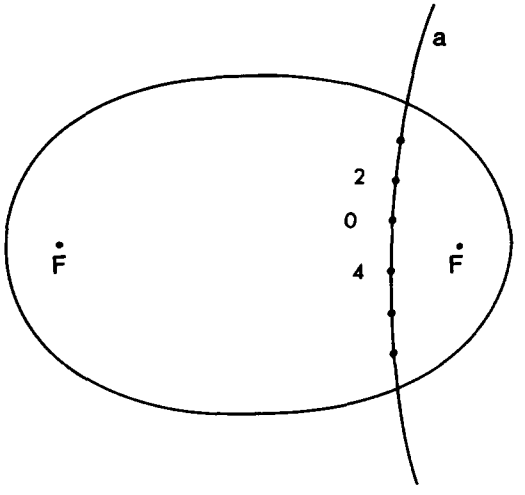

Figure 1. Grid points along the hyperbola $\xi = \xi_j$ (a).

similarly the term $O(k^3)$ in (2.21) so that finally we have the following:

$$\begin{aligned}
&\left(\tfrac{1}{4}k^2 s_1^2 - \tfrac{2}{3}k^3 \,\mathrm{e}^{-2\eta_1} \sinh 2\eta_1\right)\zeta_1 \\
&\quad = \tfrac{1}{12}s_1^2 k^2(\zeta_3 - 4\zeta_2) - \psi_2 - s_1 k\left(1 + \tfrac{3}{4}\cos\xi_1\right) \\
&\quad\quad - \tfrac{1}{6}k^3\left\{\tfrac{3}{4}s_1 \cos\xi_1 + \tfrac{3}{2}\left(\frac{\partial s}{\partial \xi}\right)_1 \sin\xi_1 - \left(\frac{\partial^2 s}{\partial \xi^2}\right)_1 \left(1 + \tfrac{3}{4}\cos\xi_1\right)\right\},
\end{aligned} \tag{2.22}$$

where s and its derivatives are evaluated from (2.5).

A potential difficulty associated with the coordinate system that we have adopted is

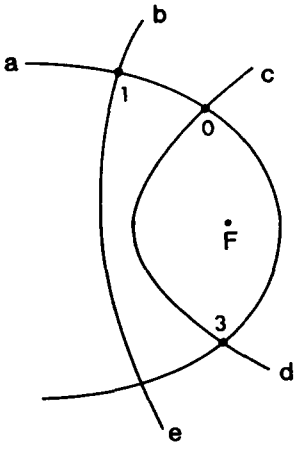

Figure 2. Grid points along the ellipse $\eta = \eta_i$ (a). The grid lines $\xi = \frac{3}{2}h$, $\xi = \frac{1}{2}h$, $\xi = (4N-1)h/2$, $\xi = (4N-3)h/2$ are shown as curves (b), (c), (d) and (e) respectively.

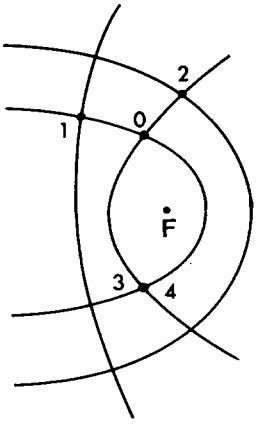

Figure 3. The grid close to a focus F showing coincidence of grid points.

that the confocal ellipses, and their hyperbolic orthogonal trajectories, degenerate to straight-line segments between, and extending from, the foci. The difficulty is overcome by ensuring that no grid point lies on this straight line. Thus we define $k = 2\eta_e/(2M-1)$ with the grid points located on the ellipses $\eta = \eta_i = (2i-1)k/2$, $i = 1, 2, \ldots, M$. This choice ensures that the grid points are equally spaced along each hyperbola which spans the ellipse. Close to the 'degenerate lines' η-derivatives are represented using the points marked 0, 2, 4 in Fig. 1. Since η increases away from the major axis the same pattern is adopted both above and below it. For the ξ-direction where $0 \leqslant \xi \leqslant 2\pi$, the same difficulty is overcome by choosing $h = \pi/N$ with the grid points located at $\xi = \xi_j = (2j-1)h/2$, $j = 1, 2, \ldots, 2N$. Close to the ends of the confocal ellipses derivatives with respect to ξ are represented using the points 0, 1, 3 in Fig. 2. This choice of grid leads to an unusual, but entirely satisfactory, situation when the point 0 at which derivatives are to be evaluated lies on the hyperbola $\xi = \frac{1}{2}h$, and the ellipse $\eta = \frac{1}{2}k$, since in that case the points we have labelled 3 and 4 in our computational mesh coincide as shown in Fig. 3.

3. Numerical procedures

In our formulation of the problem, described in Section 2 above, the sets of finite-difference equations (2.8), (2.19) can be solved, subject to their boundary conditions, by an iterative procedure. This procedure, described in more detail below, converges satisfactorily for values of the Reynolds number up to $R = 7000$. Solutions for values of R beyond this have not been considered because of the desire to maintain accuracy in the boundary layer that forms at the bounding ellipse. This satisfactory convergence may be attributed to the fact that each of the individual sets of difference equations for ψ and ζ has an associated matrix which is diagonally dominant. From the work of Varga [6] we know that for each of (2.8), (2.19), treated separately as a set of linear algebraic equations, the successive over-relaxation procedure converges for a well-defined range of the relaxation parameter. This, it appears, facilitates the convergence of an iterative procedure in which the sets of equations are solved alternately.

For each eccentricity considered, an initial distribution of $\psi = 0.0$ and $\zeta = 2.0$ was used as a starting solution for a Reynolds number typically 1000. Thereafter, a converged

solution at one Reynolds number was taken as the initial solution for an increased value of R. Each iteration cycle involves a complete sweep of the interior grid points to update ψ using (2.8), a complete sweep of the interior grid points to update ζ using (2.19), and then the computation of new values of ζ on the boundary using (2.22). We have chosen to employ line relaxation for the iterations using (2.8) and (2.19). Typically, for (2.8), a tridiagonal system of equations is formed for ψ at the grid points along the half-hyperbola $\xi = \xi_i$, $\frac{1}{2}k \leqslant \eta \leqslant \eta_e - k$, where the most recent values of ψ and ζ on adjacent half-hyperbolae are used to evaluate the right-hand side of the tridiagonal system. If ψ_0 denotes the solution of the equations at a grid point 0, and $\psi_0^{(m)}$ is the previous value at that point, a new value $\psi_0^{(m+1)}$ is computed there, using a relaxation factor ω, as

$$\psi_0^{(m+1)} = (1-\omega)\psi_0^{(m)} + \omega\psi_0. \tag{3.1}$$

In general it was found that the relaxation factor in (3.1) and the corresponding factors associated with (2.19) and (2.22), had to be smaller than unity in order to maintain stability, and frequently we used factors of 0.8.

The iteration cycle described above is repeated until convergence is achieved, which is defined by the criteria

$$\begin{aligned} &\sum |1 - \psi^{(m+1)}(\xi, \eta)/\psi^{(m)}(\xi, \eta)| < M \times N \times 10^{-8}, \\ &\sum |1 - \zeta^{(m+1)}(\xi, \eta)/\zeta^{(m)}(\xi, \eta)| < M \times N \times 10^{-8}, \end{aligned} \tag{3.2}$$

where the summation is over all grid points. These tests and a supplementary monitoring of the vorticity at the centre of the ellipse, ensured that all flow quantities had converged to limits with a very high degree of accuracy.

All our calculations have been carried out on two grids for which $h_1 = \pi/30$, $k_1 = 2\eta_e/87$ and $h_2 = \pi/90$, $k_2 = 2\eta_e/261$; h^2-extrapolation has then been used to obtain a more accurate solution as follows. If P_1, P_2 denote a flow property on each of these grids then a more accurate estimate P_3 is obtained from the extrapolation formula $P_3 = \frac{1}{8}(9P_2 - P_1)$. The choice of the grid size is such that for the fine mesh the boundary layer at the bounding ellipse is represented by 15 to 20 grid points over the range of Reynolds numbers for which solutions have been obtained. Our calculations have been carried out for three ellipses corresponding to eccentricities $e = 0.725$, 0.77 and 0.875, and in the next section we present representative results for values of $R = 2000$ to 7000.

4. Calculated results

In his investigation of flows of the type under consideration in this paper, Riley [2] has used boundary-layer methods corresponding to the case of infinite Reynolds number. An inviscid uniform vortex core, with vorticity ζ_∞, for which

$$\psi = -2\zeta_\infty \, e^{-2\eta_e} \left(\frac{\sinh^2\eta_e \cosh^2\eta \cos^2\xi + \cosh^2\eta_e \sinh^2\eta \sin^2\xi}{\cosh^2\eta_e + \sinh^2\eta_e} \right) \tag{4.1}$$

is surrounded by its controlling viscous boundary layer. Although periodicity of the boundary-layer solution should be sufficient to determine ζ_∞ Riley shows that, because of

the finite computational domain, periodicity alone is not sufficient, and care must be taken in matching the boundary-layer and core vorticities in order to determine ζ_∞. Results were presented in [2] for a range of values of e up to $e = 0.77$. Riley was unable to

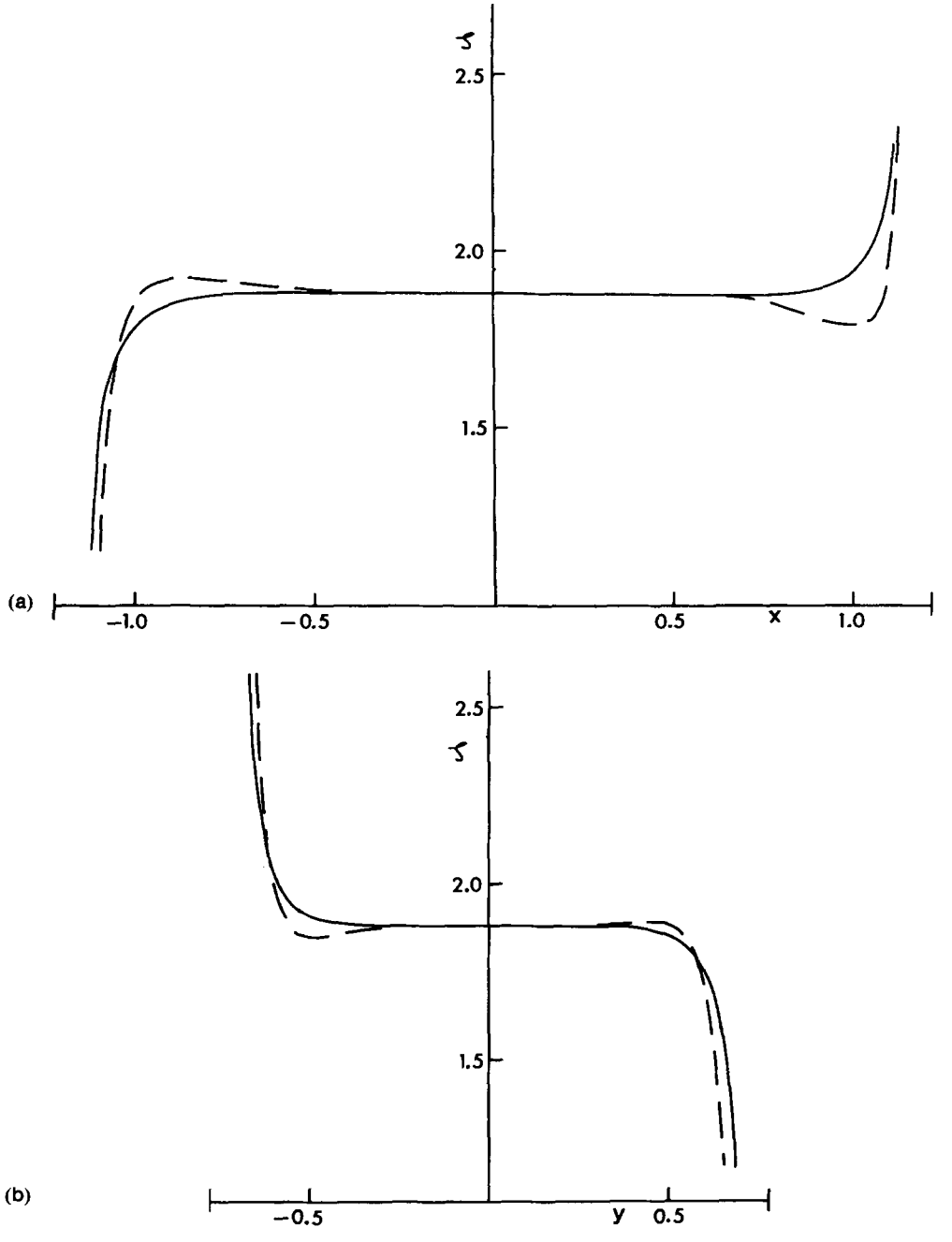

Figure 4. The variation of vorticity along (a) the major axis and (b) the minor axis of the ellipse with $e = 0.77$ for $R = 3000$ ———, $R = 2000$ - - - - - -.

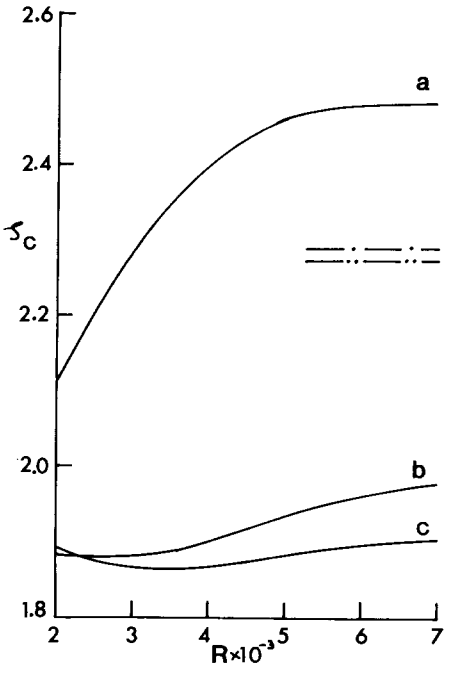

Figure 5. The variation of ζ_c with R for $e = 0.875$ (a), $e = 0.77$ (b) and $e = 0.725$ (c). The asymptotic results [2] for cases (b) and (c) are shown as $\cdot-\cdot-\cdot$, $\cdot\cdot-\cdot\cdot-\cdot\cdot$ respectively

extend his results beyond this value and attributed this failure to the development of a singularity in the solution at a point of vanishing velocity and vorticity in the boundary layer. This in turn suggested the possibility of reversed flow in the boundary layer for $e > 0.77$.

In Fig. 4 we show, for the case $e = 0.77$, the distribution of vorticity along the major and minor axes of the ellipse for the two values of $R = 2000, 3000$. Even at these Reynolds numbers there is clear evidence of the development of a core, in which the flow behaves as if it were inviscid in nature with uniform vorticity, surrounded by thin boundary layers. Since these boundary layers control the core flow it is essential that they be resolved accurately as remarked in Section 3.

In Fig. 5 we explore further the variation with R of ζ_c, defined to be the vorticity at the centre of the ellipse, up to $R = 7000$, for each of the cases $e = 0.725, 0.77, 0.875$. The results have been obtained from our coarse-grid and fine-grid solutions by h^2-extrapolation in the manner outlined in Section 3. We remark that the extrapolated and fine-grid solutions differ by never more than 2% in the core region. From Fig. 5 we see that when $e = 0.875$ the core vorticity ζ_c has effectively reached its asymptotic value, but this is not the case for the two lower values of e. We have also included in Fig. 5 the asymptotic values, in the limit $R \to \infty$, of ζ_c as predicted in [2], for the cases $e = 0.725, 0.77$. Even at $R = 7000$ the calculated values fall short of these asymptotic values by some 15%. Now, we note that neither the bounding ellipse, nor the velocity of slip (2.3) at it, has either any discontinuity or discontinuity in slope and that as a consequence we may represent ζ_c, asymptotically in the limit $R \to \infty$, as

$$\zeta_c \sim \zeta_\infty + a_0 R^{-1/2} + b_0 R^{-1}. \tag{4.2}$$

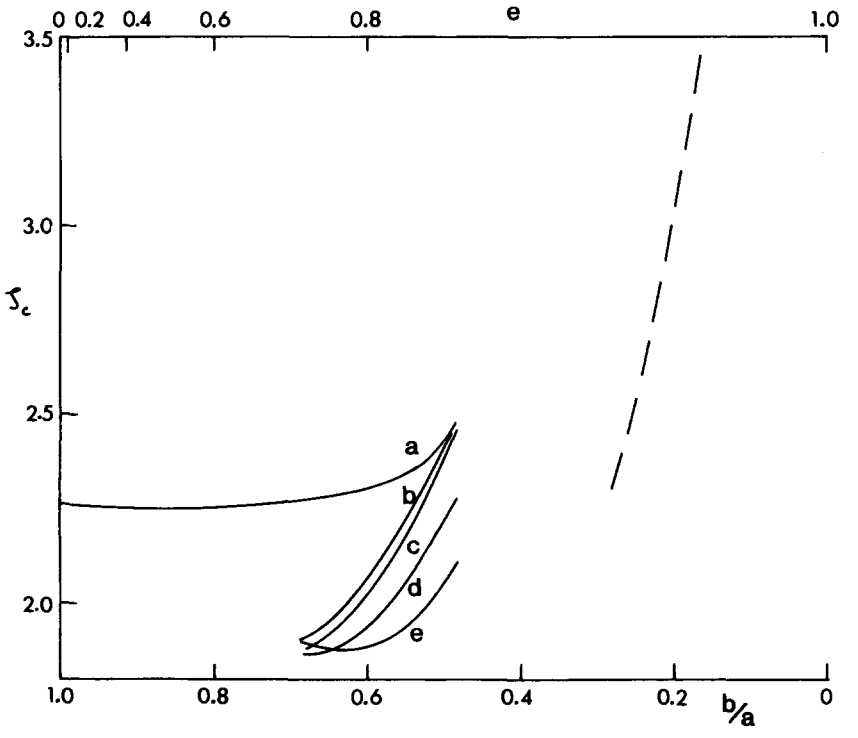

Figure 6. The variation of ζ_c with b/a (or e) for various values of the Reynolds number R. $R = \infty$ (a), $R = 7000$ (b), $R = 5000$ (c), $R = 3000$ (d) $R = 2000$ (e). The common asymptote $\zeta_c \sim \{8(1-e)\}^{-1/2} + \frac{1}{2}$ is also shown — — —.

For the values of $e = 0.725$, 0.77 we have estimated ζ_∞ using the asymptotic relation (4.2) and the three values $R = 5000$, 6000, 7000. We report that our estimates of ζ_∞ differ by less than 2% and 5% respectively from the asymptotic value obtained in [2], and shown in Fig. 5. This in turn confirms the effectiveness of the method of [2] for problems of this type in the high-Reynolds-number limit.

Figure 6 shows the variation of ζ_c both with axis ratio and eccentricity. In this figure we have included, in addition to our calculated results, the values ζ_∞ from [2], which have been extrapolated to include the value at $e = 0.875$ shown in Fig. 5. We note that in presenting these results we have been guided by our calculations at $e = 0.875$ to assume that for $e \gtrsim 0.875$ the values of ζ_∞ and ζ_c at $R = 7000$ are graphically indistinguishable. It can be shown, for all values of R, that $e = 1$ is an asymptote for the (ζ_c, e)-curves as follows. For $1 - e \ll 1$, ζ_c is easily estimated from (2.3), as velocity difference divided by distance, with $\xi = \pm \frac{1}{2}\pi$ as $\zeta_c \sim l/b \sim \{8(1-e)\}^{-1/2} + \frac{1}{2}$, a result that is independent of R. This common asymptote is also included in Fig. 6. We report no unusual features, in the solutions we have obtained, that may explain the failure of the method of [2] for $e > 0.77$ except to note, as is evident from Fig. 6, that it is in this range that $\zeta_\infty(e)$ begins to change quite rapidly.

For $e = 0.77$ boundary-layer profiles are presented in [2] at four stations around the ellipse. Using these profiles together with (4.1) we may form a composite solution which is the leading term in a uniformly-valid asymptotic solution as $R \to \infty$. In Fig. 7 we

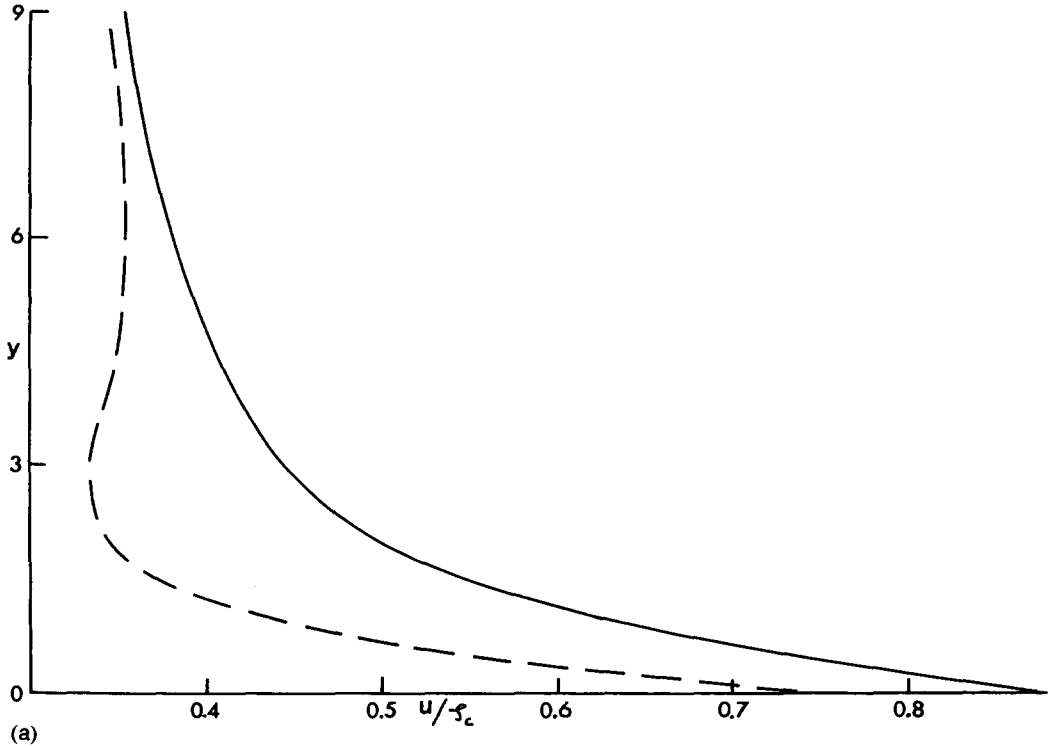

(a)

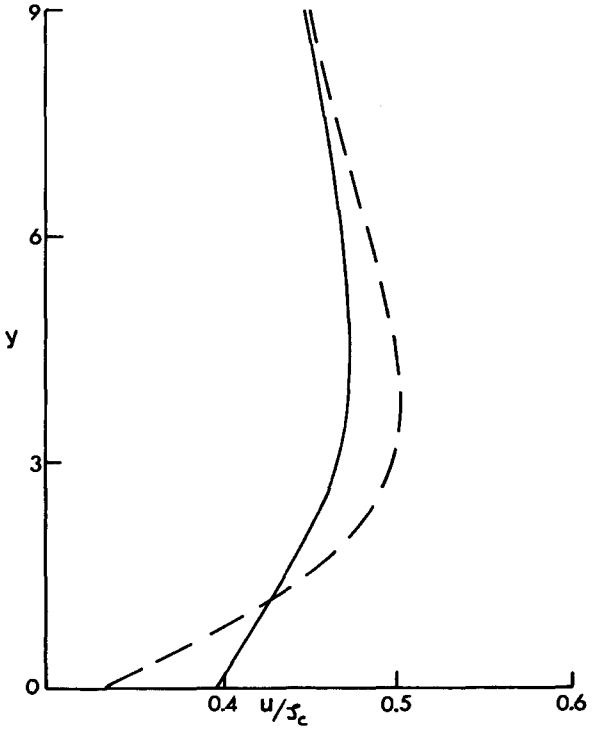

(b)

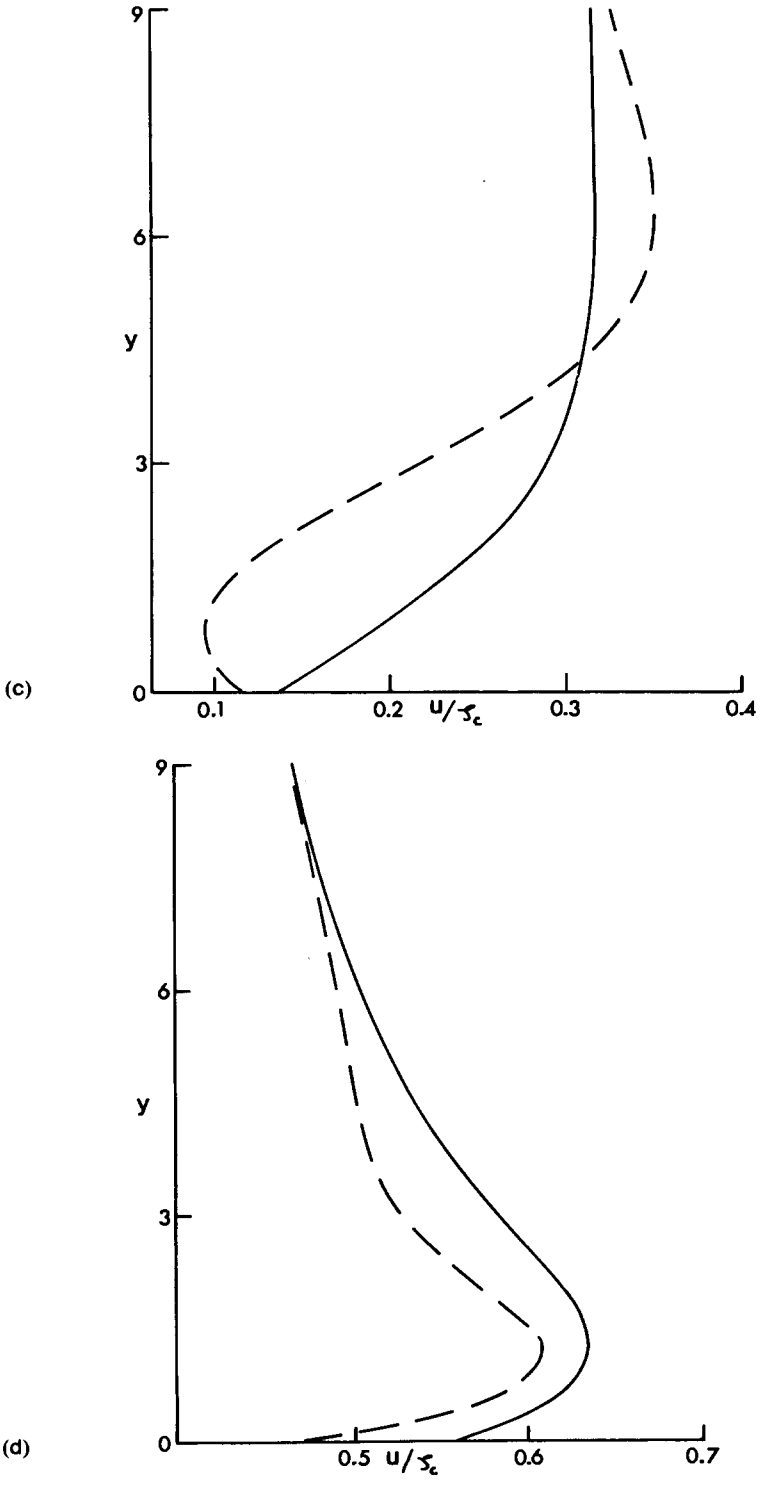

Figure 7. Profiles of u/ζ_c at $R = 5000$ ———, and a one-term uniformly valid solution derived from [2] at $R = \infty$ — — —. (a) $\xi = 4\pi/30$, (b) $\xi = 18\pi/30$, (c) $\xi = 32\pi/30$, (d) $\xi = 46\pi/30$.

compare, at $R = 5000$, these uniformly valid profiles with the profiles calculated by the methods of this paper. Because of the significant differences in ζ_c (see Fig. 5) we have thought it appropriate to compare u/ζ_c in each case. We note that at two stations the features of the asymptotic profiles are represented quite well by our calculations, but not at the other two stations. This provides further evidence that $R = 5000$ is not large in an asymptotic sense for this value of e and, furthermore, suggests that different parts of the flow field approach their asymptotic limits at different rates as R increases.

5. Conclusions

By considering numerical solutions of the steady, two-dimensional Navier-Stokes equations in an elliptical geometry we have further demonstrated the applicability and effectiveness of the powerful numerical method introduced by Dennis and Hudson [3]. For our flow with closed streamlines we have shown the emergence, as the Reynolds number increases, of a region of flow in which the vorticity is uniform, separated from the boundary by thin boundary layers. We have extracted asymptotic information, for large Reynolds number, from our solutions that compares favourably with the asymptotic results of Riley [2]; this in turn demonstrates the effectiveness of the approach of [2] to these problems in the limit of infinite Reynolds number.

References

[1] G.K. Batchelor, *An Introduction to Fluid Dynamics*, Cambridge University Press (1967).
[2] N. Riley, High Reynolds number flows with closed streamlines, *J. Engg. Math.* 15 (1981) 15–27.
[3] S.C.R. Dennis and J.D. Hudson, A difference method for solving the Navier-Stokes equations, *Proc. Ist Int. Conf. on Numerical Methods in Laminar and Turbulent Flow*, Pentech Press, London (1978) 69–80.
[4] S.C.R. Dennis, Calculation of the steady flow through a curved tube using a new finite-difference method, *J. Fluid Mech.* 99 (1980) 449–467.
[5] S.C.R. Dennis, Finite differences associated with second-order differential equations, *Quart. Jl. Mech. Appl. Math.* 13 (1960) 487–507.
[6] R.S. Varga, *Matrix Iterative Analysis*, Prentice-Hall (1962).
[7] L.C. Woods, A note on the numerical solution of fourth-order differential equations. *Aero. Quart.* 5 (1954) 176–184.